ACS Medicinal Chemistry Letters

Letter

pubs.acs.org/acsmedchemlett

Synthesis of [^{11}C]Bexarotene by Cu-Mediated [^{11}C]Carbon Dioxide Fixation and Preliminary PET Imaging

Benjamin H. Rotstein,[†,‡] Jacob M. Hooker,[‡,§] Jiyeon Woo,[†] Thomas Lee Collier,[†,‡,∥] Thomas J. Brady,[†,‡] Steven H. Liang,*[,†,‡] and Neil Vasdev*[,†,‡]

[†]Division of Nuclear Medicine and Molecular Imaging & Center for Advanced Medical Imaging Sciences, Massachusetts General Hospital, Boston, Massachusetts 02114, United States

[‡]Department of Radiology, Harvard Medical School, Boston, Massachusetts 02114, United States

[§]Athinoula A. Martinos Center for Biomedical Imaging, Massachusetts General Hospital, Charlestown, Massachusetts 02129, United States

[∥]Advion, Inc., Ithaca, New York 14850, United States

Supporting Information

ABSTRACT: Bexarotene (Targretin) is a retinoid X receptor (RXR) agonist that has applications for treatment of T cell lymphoma and proposed mechanisms of action in Alzheimer's disease that have been the subject of recent controversy. Carbon-11 labeled bexarotene ([^{11}C-*carbonyl*]4-[1-(3,5,5,8,8-pentamethyltetralin-2-yl)ethenyl]benzoic acid) was synthesized using a Cu-mediated cross-coupling reaction employing an arylboronate precursor **1** and [^{11}C]carbon dioxide under atmospheric pressure in 15 ± 2% uncorrected radiochemical yield (n = 3), based on [^{11}C]CO_2. Judicious choice of solvents, catalysts, and additives, as well as precursor concentration and purity of [^{11}C]CO_2, enabled the preparation of this ^{11}C-labeled carboxylic acid. Formulated [^{11}C]bexarotene was isolated (>37 mCi) with >99% radiochemical purity in 32 min. Preliminary positron emission tomography−magnetic resonance imaging revealed rapid brain uptake in nonhuman primate in the first 75 s following intravenous administration of the radiotracer (specific activity >0.3 Ci/μmol at time of injection), followed by slow clearance (Δ = −43%) over 60 min. Modest uptake (SUV_{max} = 0.8) was observed in whole brain and regions with high RXR expression.

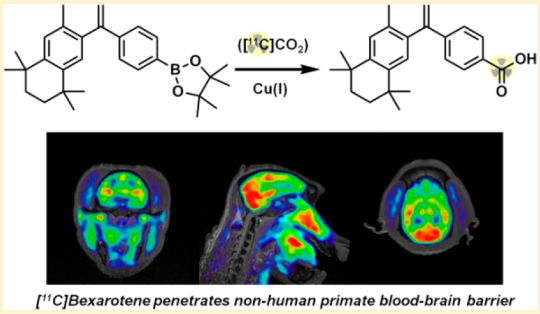

KEYWORDS: *Bexarotene, targretin, positron emission tomography, carbon-11, carbon dioxide fixation, retinoid X receptor, Alzheimer's disease*

Retinoid X receptors (RXRs) function as key transcription factors inasmuch as they are the heterodimeric partners for most nuclear receptors, including retinoic acid receptors (RARs), peroxisome proliferator-activated receptors (PPARs), vitamin D receptor, and thyroid hormone receptor.[1] Retinoid X ligands (e.g., 9-*cis* retinoic acid, Figure 1) are small lipophilic hormones, which, when bound to a heterodimeric or a homodimeric (i.e., RXR-RXR fusion) receptor, cause it to bind a transcription complex on DNA and to promote expression of target genes. RXRs are found ubiquitously and differentially in mammalian cells, including in both glial and neuronal brain tissue.[2] Defective retinoid signaling and deficiency of apolipoprotein E (ApoE) are closely associated with Alzheimer's disease (AD).[3]

Bexarotene (4-[1-(3,5,5,8,8-pentamethyltetralin-2-yl)-ethenyl]benzoic acid, Figure 1), an FDA-approved selective RXR agonist,[4] has recently been demonstrated to induce clearance of β-amyloid from the brains of murine AD models through activation of the *APOE* gene, which is the most indicative genetic risk factor for late-onset AD.[5] In vitro and in vivo studies also suggest that bexarotene is acting on RXRs, and not directly on β-amyloid or by compromising the blood−brain barrier.[6] A transgenic mouse model of AD (Tg2576) exhibited reversal of cognitive and behavioral degradation with the administration of bexarotene.[5] These findings have proven to be controversial, however, as several laboratories have struggled to reproduce both the scope and magnitude of the in vivo results.[7−11] An additional caveat to these results is that the bexarotene dose used to achieve these effects with sufficient brain penetration (100 mg/kg/day, po) translates to about three times that of the clinical dose.[12] It is noteworthy that the brain permeability of bexarotene has only been evaluated in mouse models. Nevertheless, in advance of clinical trials and in the absence of effective treatments, off-label demand for bexarotene among patients and families suffering from AD poses an ethical quandary.[13] To help guide drug repositioning,

Received: February 10, 2014
Accepted: February 27, 2014
Published: February 27, 2014

 © 2014 American Chemical Society

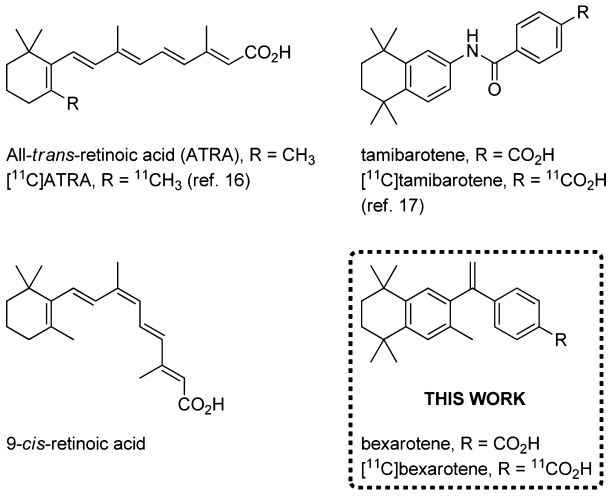

Figure 1. Top: Structures of RAR-selective agonists all-*trans*-retinoic acid and tamibarotene (Am 80) (for carbon-11 isotopologues see refs 16 and 17). Bottom: Structures of RXR-selective agonists 9-*cis*-retinoic acid and bexarotene.

there is an urgent need to evaluate the brain pharmacokinetics of this pharmaceutical in higher species.

Carbon-11 (^{11}C; $t_{1/2}$ = 20.4 min) labeled radiotracers are used extensively to study pharmacokinetics of drug compounds in vivo via positron emission tomography (PET), a sensitive and noninvasive molecular imaging modality.[14,15] In the present study, we describe an efficient synthesis of [^{11}C]bexarotene by rapid Cu-mediated [^{11}C]CO_2-fixation using an arylboronate precursor, thereby preparing the isotopologue at the carbonyl position of the corresponding carboxylic acid. We further carried out a preliminary PET–magnetic resonance (PET–MR) imaging study in a nonhuman primate with this radiotracer to determine brain uptake and biodistribution of this labeled drug.

Cyclotron generated carbon-11 is most commonly produced in the form of [^{11}C]carbon dioxide and is subsequently converted to reactants such as [^{11}C]methyl iodide or [^{11}C]methyl triflate. [^{11}C]All-*trans*-retinoic acid has been prepared using [^{11}C]CH_3I,[16] and [^{11}C]tamibarotene, another retinoid-based therapeutic, has been prepared by a multistep approach via [^{11}C]CO (Figure 1).[17] In the latter example, methoxycarbonylation of arylboronates was achieved using a Pd(0)-mediated reaction with [^{11}C]CO, and the products were subsequently hydrolyzed to generate [^{11}C]carboxylic acids.[17] This methodology requires both the conversion of cyclotron-generated [^{11}C]CO_2 to [^{11}C]CO prior to the labeling reaction and cooling of the reaction mixture to −15 °C to improve trapping of [^{11}C]CO in organic solvents.

In contrast, we and others have been active in development of new methodologies for direct fixation of [^{11}C]CO_2 in the synthesis of complex radiolabeled molecules and tracers (for a recent review see ref 18). Mild methodologies that rely on organic bases to trap [^{11}C]CO_2 in solution prior to covalent bond formation have been developed to access [^{11}C]ureas, [^{11}C]carbamates, [^{11}C]oxazolidinones, and [^{11}C]carboxylic acids.[18] Carboxylation of Grignard or organolithium reagents with [^{11}C]CO_2 represents a direct route to ^{11}C-labeled carboxylic acids. However, applications of this approach have been limited to simple labeling precursors due to the high reactivity of organometallic reagents. Rigorous exclusion of atmospheric moisture and CO_2 during storage and manipulation is necessary to obtain labeled products with consistently high radiochemical yields and specific activities. By way of preparing [^{11}C]carboxylic acids, a copper(I)-mediated carboxylation of arylboronates using [^{11}C]CO_2 and KF/crypt-222 additives was recently reported.[19]

The synthesis of [^{11}C]bexarotene was achieved by the reaction of [^{11}C]CO_2 with boronic ester precursors **1** (Table 1), without intermediate chemical transformations. Pinacol arylboronic ester **1a** was synthesized in four steps (36% overall yield) from toluene.[20] [^{11}C]CO_2 was extracted from cyclotron

Table 1. Optimization of Reaction Conditions for the Synthesis of [^{11}C]Bexarotene

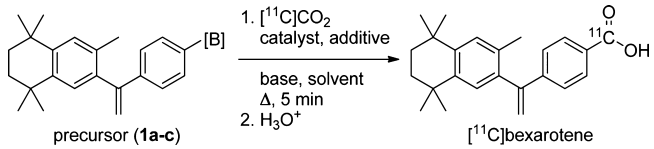

entry	[B][a]	catalyst	additive	base	solvent	temp (°C)	conv[b] (%)
1	Bpin (**1a**)	CuI	KF/crypt-222	TMEDA	DMF	100	9
2	**1a**	CuI	KF/crypt-222	TMEDA, DBU	DMF	100	NR
3	**1a**	CuI	KF/crypt-222	TMEDA, BEMP	DMF	100	NR
4	**1a**	CuTC	KF/crypt-222	TMEDA	DMF	100	22
5	**1a**	CuTC	TBAT	TMEDA	DMF	100	25
6	**1a**	CuTC	TBAT	TMEDA	NMP	100	34
7	$B(OH)_2$ (**1b**)	CuTC	TBAT	TMEDA	NMP	100	NR
8	BF_3K (**1c**)	CuTC	TBAT	TMEDA	NMP	100	NR
9	**1a**	CuTC	TBAT	TMEDA	NMP	120	8
10	**1a**	CuTC	TBAT	TMEDA	NMP	90	18
11[c]	**1a**	CuTC	TBAT	TMEDA	NMP	100	39
12	**1a**[d]	CuTC	TBAT	TMEDA	NMP	100	86
13[e]	**1a**[d]	CuTC	TBAT	TMEDA	NMP	100	88

[a]Unless otherwise noted, precursor concentration was 0.03 M. [b]Determined by radioHPLC integration of product peaks and unreacted [^{11}C]CO_2 complexes. No other radioactive products were observed. [c]Reaction was heated for 10 min. [d]Precursor concentration was 0.15 M. [e]Added butylated hydroxytoluene (BHT, 10 mol % relative **1a**). Bpin, pinacolatoboron

dx.doi.org/10.1021/ml500065q | ACS Med. Chem. Lett. 2014, 5, 668–672

target gas in a liquid N_2-cooled trap and subsequently bubbled into a reactor vial containing the labeling precursor **1**, solvent, catalyst, additives, and fixating base. Preliminary experiments revealed that 1,8-diazabicyclo[5.4.0]undec-7-ene (DBU) and 2-*tert*-butylimino-2-diethylamino-1,3-dimethylperhydro-1,3,2-diazaphosphorine (BEMP), though efficient for trapping $[^{11}C]CO_2$ in solution,[21,22] were incompatible with the Cu-mediated coupling (Table 1, entries 1−3). Using *N*,*N*,*N*′,*N*′-tetramethylethylenediamine (TMEDA) as base and ligand for the metal center, modest conversion was observed. We found that the more soluble copper(I) thiophene-2-carboxylate (CuTC) was an improvement over CuI, and replacing KF/crypt-222 with crystalline and bench-stable tetrabutylammonium difluorotriphenylsilicate (TBAT) led to more consistent reaction outcomes (entry 5). To improve precursor and catalyst solubility the solvent was changed from *N*,*N*-dimethylformamide (DMF) to *N*-methylpyrrolidinone (NMP) (entry 6). Radiochemical conversion remained suboptimal, however, so we turned to alternative precursors to improve on the pinacol ester **1a**.

To our dismay, boronic acid **1b** and potassium trifluoroborate **1c**, each prepared in a single step from **1a**, were unreactive in this context (entries 7 and 8). Higher temperatures were unable to afford greater conversion, and longer reaction times did not prove to be fruitful (entries 9−11). Significant improvements were realized by increasing the concentration of precursor in the reaction mixture from 0.03 to 0.15 M, which led to high radiochemical conversion to product (86% relative unreacted $[^{11}C]CO_2$ and solvates, entry 12). As the added precursor did not threaten to complicate purification of $[^{11}C]$bexarotene, we concluded that the optimal conditions for radiolabeling were **1a** (0.15 M), CuTC (0.015 M), TBAT (0.02 M), TMEDA (1.33 M), NMP, and $[^{11}C]CO_2$, heated for 5 min at 100 °C at atmospheric pressure.

As several oxidation states and mechanisms are available to copper-catalyzed coupling reactions, we sought to gain insight into the operative mode of reactivity. Reactions were run at our optimized conditions for preparation of $[^{11}C]$bexarotene with the addition of radical inhibitor butylated hydroxytoluene (BHT). At substoichiometric (10 mol % relative to precursor **1a**) concentrations of BHT, little change in radiochemical conversion (88%, Table 1, entry 13) was observed compared to our optimized conditions. This evidence supports nonradical mechanisms for synthesis of $[^{11}C]$bexarotene by copper-mediated $[^{11}C]CO_2$-fixation.

Based on the optimized conditions described above, the reaction was scaled and $[^{11}C]$bexarotene was isolated and formulated for preclinical imaging studies. Briefly, after bubbling $[^{11}C]CO_2$ into the reaction mixture, the vial was sealed and heated to 100 °C for 5 min, after which the reaction was quenched with HPLC mobile phase (80% CH_3CN, 20% 0.1 M $NH_4{\cdot}HCO_{2(aq)}$) and purified by semipreparative HPLC. Reformulation of the product HPLC fraction into ethanolic saline and sterile filtration provided $[^{11}C]$bexarotene in injectable form. The non-decay-corrected isolated radiochemical yield (RCY) based on $[^{11}C]CO_2$ was 15 ± 2%, after 32 ± 3 min synthesis time (n = 3). Radiochemical purity was >99% for each synthesis.

To determine the in vivo distribution and brain permeability of $[^{11}C]$bexarotene, we performed PET imaging in an isoflurane-anesthetized baboon (3 y.o., 16.4 kg, female). Bolus iv administration of $[^{11}C]$bexarotene (4.14 mCi; with specific activity of 310 mCi/μmol at time of injection) was coincident with initiation of a 60 min dynamic brain PET acquisition and followed by abdominal and thoracic static PET scans to determine biodistribution. $[^{11}C]$Bexarotene rapidly crossed the BBB and reached a maximum whole brain activity of 0.8 SUV (standardized uptake value) at approximately 90 s post injection (Figure 2). A second, slightly lower peak was

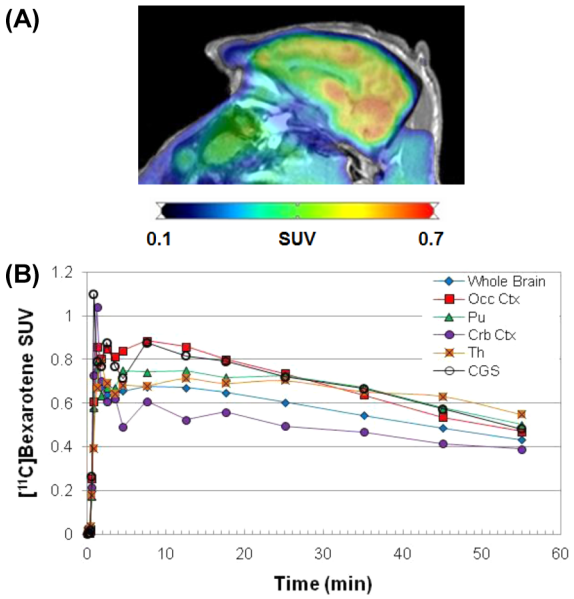

Figure 2. Nonhuman primate PET imaging: (A) Summed image 15−60 min post tracer injection. (B) Time−activity curve for whole-brain and selected brain regions. For ROI placement, see Supporting Information. Occ Ctx, occipital cortex; Pu, putamen; Crb Ctx, cerebral cortex; Th, thalamus; CGS, cingulate sulcus; SUV, standardized uptake value.

reached near 8 min postinjection. Regional brain distribution was fairly uniform, with greater uptake in the occipital cortex, putamen, and thalamus. Likewise, RXR distribution is known to be enriched in the rhombencephalon and the basal ganglia.[2] The log$D_{7.4}$ of $[^{11}C]$bexarotene was measured to be 3.68.[23] which likely accounts for the slow clearance (Δ = −43%) observed over 60 min. Abdominal and thoracic PET data revealed high activity in the heart (>35 SUV), gall bladder (>20 SUV), and small intestine (>50 SUV) and accumulation in the liver, consistent with high levels of RXR expression in the heart and liver, as well as biliary metabolism and excretion.[24,25] To our knowledge this work represents the first $[^{11}C]$carboxylic acid radiotracer synthesized from $[^{11}C]CO_2$ suitable for use in PET imaging studies without using organometallic precursors.

In summary, we have optimized a copper-mediated $[^{11}C]CO_2$-fixation reaction for the synthesis of $[^{11}C]$-bexarotene. Cu-mediated $[^{11}C]$carboxylation of arylboronates is an efficient and direct route to $[^{11}C]$carboxylic acids that obviates the need for preformed and unstable organometallic reagents or multistep synthetic strategies, and should be broadly applicable toward the synthesis of ^{11}C-labeled carboxylic acids and retinoid-based imaging agents. Preclinical PET imaging using $[^{11}C]$bexarotene demonstrated a reasonable brain uptake in nonhuman primate and shows regional distribution in line with known RXR distribution. $[^{11}C]$-Bexarotene has potential to be used for pharmacokinetic and dose response studies and warrants further imaging studies that could facilitate clinical translation.

dx.doi.org/10.1021/ml500065q | ACS Med. Chem. Lett. 2014, 5, 668−672

EXPERIMENTAL PROCEDURES

Radiosynthesis of [^{11}C]Bexarotene. Prior to end-of-bombardment, a septum-sealed vial was charged with pinacol arylboronate **1a** (12.9 mg), CuTC (1.0 mg), TBAT (2.7 mg), TMEDA (60 μL), and NMP (300 μL) and agitated to ensure complete solubility of its contents. Cyclotron-generated [^{11}C]CO_2 was trapped in a short metal coil, cooled in a liquid N_2 bath, and then bubbled into the reaction mixture with $He_{(g)}$ at 10 mL/min. When radioactivity had peaked, gas flow was halted, and the vial was sealed and heated to 100 °C for 5 min. The reaction mixture was then quenched with 1 mL of HPLC mobile phase (80% CH_3CN, 20% 0.1 M $NH_4{\cdot}HCO_{2(aq)}$) and purified by semipreparative HPLC.

ASSOCIATED CONTENT

Supporting Information

Full experimental details and characterization data for organic and radiochemical procedures, PET imaging studies, and log*D* determination. This material is available free of charge via the Internet at http://pubs.acs.org.

AUTHOR INFORMATION

Corresponding Author

*Tel: +1 617 643 4736. Fax: +1 617 726 6165. E-mail: liang.steven@mgh.harvard.edu and vasdev.neil@mgh.harvard.edu.

Funding

B.H.R. is a Natural Sciences and Engineering Research Council of Canada (NSERC) Postdoctoral Fellow.

Notes

The authors declare no competing financial interest.

ACKNOWLEDGMENTS

We thank David F. Lee, Jr., Dr. Ronald Moore, Nathan Schauer, and Ehimen Aisaborhale for assistance with radioisotope production and Dr. Ronald Borra, Shirley Hsu, Grae Arabasz, and Helen Deng for assistance with PET-MR imaging experiments.

DEDICATION

This article is dedicated to Professor James H. Thrall on the occasion of his retirement as Chair of Radiology, Massachusetts General Hospital and Harvard Medical School.

ABBREVIATIONS

ApoE, apolipoprotein E; BBB, blood−brain barrier; CNS, central nervous system; CuTC, copper thiophene-2-carboxylate; crypt-222, 2.2.2-cryptand; DMF, *N*,*N*-dimethylformamide; NMP, *N*-methyl-2-pyrolidinone; PET, positron emission tomography; PPAR, peroxisome proliferator-activated receptor; RAR, retinoic acid receptor; RXR, retinoid X receptor; SUV, standardized uptake value; TBAT, tetrabutylammonium triphenyldifluorosilicate; TMEDA, *N*,*N*,*N*′,*N*′-tetramethylethylenediamine

REFERENCES

(1) Huang, P.; Chandra, V.; Rastinejad, F. Retinoic Acid Actions through Mammalian Nuclear Receptors. *Chem. Rev.* **2014**, *114*, 233−254.

(2) Moreno, S.; Farioli-Vecchioli, S.; Cerù, M. P. Immunolocalization of Peroxisome Proliferator-Activated Receptors and Retinoid X Receptors in the Adult Rat CNS. *Neuroscience* **2004**, *123*, 131−145.

(3) Goodman, A. B.; Pardee, A. B. Evidence for Defective Retinoid Transport and Function in Late Onset Alzheimer's Disease. *Proc. Natl. Acad. Sci. U.S.A.* **2003**, *100*, 2901−2905.

(4) Boehm, M. F.; Zhang, L.; Badea, B. A.; White, S. K.; Mais, D. E.; Berger, E.; Suto, C. M.; Goldman, M. E.; Heyman, R. A. Synthesis and Structure-Activity Relationships of Novel Retinoid X Receptor-Selective Retinoids. *J. Med. Chem.* **1994**, *37*, 2930−2941.

(5) Cramer, P. E.; Cirrito, J. R.; Wesson, D. W.; Lee, C. Y. D.; Karlo, J. C.; Zinn, A. E.; Casali, B. T.; Restivo, J. L.; Goebel, W. D.; James, M. J.; Brunden, K. R.; Wilson, D. A.; Landreth, G. E. ApoE-Directed Therapeutics Rapidly Clear β-Amyloid and Reverse Deficits in AD Mouse Models. *Science* **2012**, *335*, 1503−1506.

(6) Bachmeier, C.; Beaulieu-Abdelahad, D.; Crawford, F.; Mullan, M.; Paris, D. Stimulation of the Retinoid X Receptor Facilitates Beta-Amyloid Clearance Across the Blood−Brain Barrier. *J. Mol. Neurosci.* **2012**, *49*, 270−276.

(7) Fitz, N. F.; Cronican, A. A.; Lefterov, I.; Koldamova, R. Comment on "ApoE-Directed Therapeutics Rapidly Clear β-Amyloid and Reverse Deficits in AD Mouse Models". *Science* **2013**, *340*, 924−924.

(8) Price, A. R.; Xu, G.; Siemienski, Z. B.; Smithson, L. A.; Borchelt, D. R.; Golde, T. E.; Felsenstein, K. M. Comment on "ApoE-Directed Therapeutics Rapidly Clear β-Amyloid and Reverse Deficits in AD Mouse Models". *Science* **2013**, *340*, 924−924.

(9) Tesseur, I.; Lo, A. C.; Roberfroid, A.; Dietvorst, S.; Van Broeck, B.; Borgers, M.; Gijsen, H.; Moechars, D.; Mercken, M.; Kemp, J.; D'Hooge, R.; De Strooper, B. Comment on "ApoE-Directed Therapeutics Rapidly Clear β-Amyloid and Reverse Deficits in AD Mouse Models". *Science* **2013**, *340*, 924−924.

(10) Veeraraghavalu, K.; Zhang, C.; Miller, S.; Hefendehl, J. K.; Rajapaksha, T. W.; Ulrich, J.; Jucker, M.; Holtzman, D. M.; Tanzi, R. E.; Vassar, R.; Sisodia, S. S. Comment on "ApoE-Directed Therapeutics Rapidly Clear β-Amyloid and Reverse Deficits in AD Mouse Models". *Science* **2013**, *340*, 924−924.

(11) Landreth, G. E.; Cramer, P. E.; Lakner, M. M.; Cirrito, J. R.; Wesson, D. W.; Brunden, K. R.; Wilson, D. A. Response to Comments on "ApoE-Directed Therapeutics Rapidly Clear β-Amyloid and Reverse Deficits in AD Mouse Models". *Science* **2013**, *340*, 924−924.

(12) Corbett, A.; Pickett, J.; Burns, A.; Corcoran, J.; Dunnett, S. B.; Edison, P.; Hagan, J. J.; Holmes, C.; Jones, E.; Katona, C. Drug Repositioning for Alzheimer's Disease. *Nat. Rev. Drug Discovery* **2012**, *11*, 833−846.

(13) Lowenthal, J.; Hull, S. C.; Pearson, S. D. The Ethics of Early Evidence—Preparing for a Possible Breakthrough in Alzheimer's Disease. *N. Engl. J. Med.* **2012**, *367*, 488−490.

(14) Ametamey, S. M.; Honer, M.; Schubiger, P. A. Molecular Imaging with PET. *Chem. Rev.* **2008**, *108*, 1501−1516.

(15) Miller, P. W.; Long, N. J.; Vilar, R.; Gee, A. D. Synthesis of ^{11}C, ^{18}F, ^{15}O, and ^{13}N Radiolabels for Positron Emission Tomography. *Angew. Chem., Int. Ed.* **2008**, *47*, 8998−9033.

(16) Suzuki, M.; Takashima-Hirano, M.; Watanabe, C.; Ishii, H.; Sumi, K.; Koyama, H.; Doi, H. Synthesis of [^{11}C]all-*trans*-Retinoic Acid via an Alkenylboron Precursor by Pd(0)-Mediated Rapid *C*-[^{11}C]methylation. *J. Labelled Compd. Radiopharm.* **2011**, *54*, S92.

(17) Takashima-Hirano, M.; Ishii, H.; Suzuki, M. Synthesis of [^{11}C]Am80 via Novel Pd(0)-Mediated Rapid [^{11}C]Carbonylation Using Arylboronate and [^{11}C]Carbon Monoxide. *ACS Med. Chem. Lett.* **2012**, *3*, 804−807.

(18) Rotstein, B. H.; Liang, S. H.; Holland, J. P.; Collier, T. L.; Hooker, J. M.; Wilson, A. A.; Vasdev, N. $^{11}CO_2$ Fixation: A Renaissance in PET Radiochemistry. *Chem. Commun.* **2013**, *49*, 5621−5629.

(19) Riss, P. J.; Lu, S.; Telu, S.; Aigbirhio, F. I.; Pike, V. W. Cu^{I}-Catalyzed ^{11}C Carboxylation of Boronic Acid Esters: A Rapid and Convenient Entry to ^{11}C-Labeled Carboxylic Acids, Esters, and Amides. *Angew. Chem., Int. Ed.* **2012**, *51*, 2698−2702.

(20) Sarshar, S. Novel Therapeutic Agents for the Treatment of Cancer, Metabolic Diseases and Skin Disorders. WO2007022437 (A2), February 22, 2007.

(21) Hooker, J. M.; Reibel, A. T.; Hill, S. M.; Schueller, M. J.; Fowler, J. S. One-Pot, Direct Incorporation of [^{11}C]CO_2 into Carbamates. *Angew. Chem., Int. Ed.* **2009**, *48*, 3482−3485.

(22) Wilson, A. A.; Garcia, A.; Houle, S.; Vasdev, N. Direct Fixation of [^{11}C]-CO_2 by Amines: Formation of [^{11}C-*carbonyl*]-Methylcarbamates. *Org. Biomol. Chem.* **2010**, *8*, 428−432.
(23) Wilson, A. A.; Jin, L.; Garcia, A.; DaSilva, J. N.; Houle, S. An Admonition When Measuring the Lipophilicity of Radiotracers Using Counting Techniques. *Appl. Radiat. Isot.* **2001**, *54*, 203−208.
(24) Cullingford, T. E.; Bhakoo, K.; Peuchen, S.; Dolphin, C. T.; Patel, R.; Clark, J. B. Distribution of mRNAs Encoding the Peroxisome Proliferator-Activated Receptor α, β, and γ and the Retinoid X Receptor α, β, and γ in Rat Central Nervous System. *J. Neurochem.* **1998**, *70*, 1366−1375.
(25) Howell, S. R.; Shirley, M. A.; Grese, T. A.; Neel, D. A.; Wells, K. E.; Ulm, E. H. Bexarotene Metabolism in Rat, Dog, and Human, Synthesis of Oxidative Metabolites, and in Vitro Activity at Retinoid Receptors. *Drug Metab. Dispos.* **2001**, *29*, 990−998.